Histol Histopathol (2024) 39: 345-355

Histology and Histopathology
From Cell Biology to Tissue Engineering

ORIGINAL ARTICLE Open Access

MiR-5590-3p inhibits the proliferation and invasion of ovarian cancer cells through mediating the Wnt/β-catenin signaling pathway by targeting TNIK

Xiaoling Wu[1], Youwen Zhong[2], Hua Zhang[1] and Mu Li[1]

[1]Department of Obstetrics and Gynecology, the Second Affiliated Hospital of Xi'an Jiaotong University and [2]School of Economics and Finance, Xi'an Jiaotong University, Xi'an, Shaanxi, China

Summary. MicroRNAs (miRNAs) are crucial regulatory molecules involved in diverse biological processes and human diseases, including ovarian cancer (OC). miR-5590-3p has been involved in multiple malignant solid tumors, but its exact role in the progression of OC is largely unknown. This study mainly focuses on how miR-5590-3p works in OC and illuminating the underlying mechanism. We found that miR-5590-3p was significantly downregulated in human OC cell lines and patient tissues. Cell counting 8 (CCK-8) and Transwell assays proved that overexpression or inhibition of miR-5590-3p suppressed or promoted cell proliferation and cell invasion. Subsequently, TNIK was identified as a target of miR-5590-3p. Silence of TNIK by small interfering RNA (siRNA) reversed the increasing effect of miR-5590-3p inhibition on cell proliferation and invasion in OC cell lines. Furthermore, our results showed that the Wnt/β-catenin pathway was inhibited by its specific inhibitor XAV-939, but miR-5590-3p inhibitor and adenoviral TNIK overexpression vector (Ad-TNIK) reactivated the activation of Wnt/β-catenin signaling and increased cell malignancy. Lastly, tumorigenicity assay demonstrated that inhibition of miR-5590-3p increased tumor volume and weight *in vivo*. In conclusion, miR-5590-3p may function as a cancer suppressor gene in OC progression through the Wnt/β-catenin signaling by transcriptionally suppressing TNIK expression, which provides a potential therapeutic approach for ovarian cancer treatment.

Key words: Ovarian cancer (OC), miR-5590-3p, TNIK, Wnt/β-catenin signaling pathway

Corresponding Author: Xiaoling Wu, Department of Obstetrics and Gynecology, the Second Affiliated Hospital of Xi'an Jiaotong University, No. 157 Xiwu Road, Xi'an, Shaanxi 710004, China. e-mail: xiaoling_wuxl@163.com

www.hh.um.es. DOI: 10.14670/HH-18-636

Introduction

Ovarian cancer (OC) is one of the most common gynecologic malignancies, accounting for about 25%, which is ranked fifth among all cancers (Ren et al., 2015). The incidence rate has been increasing annually. Due to a lack of early symptoms and effective diagnostics, approximately 70% of OC patients are already in the middle or late stage at the first diagnosis with a lower survival rate (Siegel et al., 2017). Generally, the treatment strategy for OC mainly includes debulking surgery and chemotherapy composed mainly of platinum and taxane derivatives (Tang et al., 2017). New targeted therapies for anti-angiogenic drugs and bevacizumab have been introduced for the problems of patients with recurrent disease and resistance to platinum and taxane drugs (Marchetti et al., 2019). Although there has been significant progress in developing methods for OC treatment, issues such as poor response and recurrence remain the biggest obstacles to improve survival. Therefore, clarifying the underlying mechanism of OC progression to identify some new potential strategies for targeted therapies is urgently needed.

With the development of deep sequencing, some new potential strategies for targeted therapies have emerged, such as noncoding RNAs including microRNAs. MicroRNAs (miRNAs) can specifically bind to the 3'-UTR region of the target gene mRNA to regulate gene expression for mRNA degradation or translation inhibition (Sebastian et al., 2011). In recent years, accumulating evidence suggests that miRNAs are involved in regulating the key signaling pathways in various cancers, and that the changes in their expression lead to a series of phenotypes, such as proliferation, migration and invasion (Lim et al., 2005). Recent studies reported that miRNAs may be involved in OC cancer progression. For example, miR-1251-5p promoted carcinogenesis and autophagy by targeting the tumor suppressor TBCC in ovarian cancer cells (Wen et al.,

2015), miR-654-5p suppressed ovarian cancer development through impacting on MYC, WNT and AKT pathways (Majem et al., 2019), and miR-205 enhanced the progress of ovarian cancer cells through targeting ZEB1 (Niu et al., 2015). MiR-5590-3p has been previously indicated as a tumor-suppressive gene in variety of cancers. For example, miR-5590-3p was verified to suppress tumor growth by targeting the DDX5/AKT/m-TOR pathway in gastric cancer (Wu et al., 2018), and arrested cell cycle by the downregulation of TGFβ-R1, TGFβ-R2, SMAD3 and SMAD4 transcripts to negatively regulate the TGFβ/SMAD signaling pathway in breast cancer (Bakhshmand and Soltani, 2019). Moreover, Liang et al. verified that miR-5590-3p was upregulated in breast cancer tissues and cells, and inhibited cell proliferation, migration, and epithelial-mesenchymal transition by targeting YY1 (Liang et al., 2019). However, the function of miR-5590-3p in OC remains unclear.

TNIK (Traf-2 and Nck interacting kinase), the adaptor protein TRAF-2 and Nck interacting protein kinase, is an upstream factor of the mitogen-activated protein kinase signaling pathway. A recent study demonstrated that miR-5590-3p inhibition was able to activate the Wnt/β−catenin pathway in hepatocellular carcinoma (Zhang et al., 2019), and TNIK is also involved in the transmission of the Wnt/β-catenin signaling pathway (Mahmoudi et al., 2009; Gui et al., 2011), which is closely related to the development of tumors (Weston and Davis, 2002; Clevers and Nusse, 2012; Ford et al., 2016). Thus, we examined the relationship between miR-5590-3p and TNIK in OC incidence and discussed their possible biological function and molecular mechanism.

In this study, we found that miR-5590-3p was significantly downregulated in tumor tissues and OC cell lines. Further experiments demonstrated that miR-5590-3p played a suppressive role in regulating the OC cell proliferation and invasion via the Wnt/β-catenin pathway, and that TNIK, which functioned as a direct target of miR-5590-3p, weakened this effect. Finally, tumorigenicity assays in nude mice further demonstrated the effects of miR-5590-3p on tumor volume and weight.

Materials and methods

Ethics statement

All patients in this study signed an informed consent form prior to the study, and all experiments gained the approval of the Ethics Committee for Clinical Experiments at the Second Affiliated Hospital of Xi'an Jiaotong University (Xi'an, China).

Tissue samples and cell lines

A total of 40 pairs of ovarian epithelial cancer tissues and matched normal adjacent specimens were collected from 40 female patients (median age, 54 years; range, 36-76 years) who received surgical resection at the Second Affiliated Hospital of Xi'an Jiaotong University. The samples were obtained between January 2017 and March 2018. None of the patients had received any other treatment before surgery resection, including radiotherapy and chemotherapy. All tissue specimens were snap-frozen in liquid nitrogen and stored at -80°C following surgery for further study. All samples were clinically and pathologically verified.

Human ovarian cancer cell lines (A2780, SKOV3, HEY, OVCAR3 and IGROV1), the normal human ovarian epithelial cells (HOSEpiC) and HEK-293 cell were all obtained from the Shanghai Institute of Cell Biology (Shanghai, China). All the cells were cultured in Dulbecco's modified Eagle medium (DMEM; Thermo Fisher Scientific, Waltham, MA, USA) supplemented with 10% fetal bovine serum (FBS; Sigma-Aldrich) and kept at 37°C in a humidified incubator with 5% CO_2.

Cell transfection

Negative control (NC) mimic (5'-AAA AAA GAA CAA GAA AGG CAA-3'), NC inhibitor (5'-AAA AAA CAA GAA CAA ACC GAA-3'), miR-5590-3p mimic (5'-AAU AAA GUU CAU GUA UGG CAA-3'), and miR-5590-3p inhibitor (5'-UUA UUU CAA GUA CAU ACC GUU-3') were synthesized by GenScript Biotech Corp. (Nanjing, China). Scrambled siRNA (as NC siRNA) and siRNA against TNIK (TNIK siRNA) were purchased from Thermo Fisher Scientific (Waltham, MA, USA). A2780 and OVCAR3 cells were respectively seeded in 6-well plates at a density of 2×10^5 cells/mL. On reaching about 70% confluence, cell transfection was performed using Lipofectamine 2000 transfection reagent (Invitrogen, Carlsbad, CA, USA) following the the manufacturer's instructions. Cells were collected at 48h after transfection, and the transfection efficiency was determined by Western blotting or qPCR.

Western blotting analysis

Cells or tumor tissue homogenates were incubated with the RIPA Lysis Buffer (Millipore) on ice for 10 min, and then collected into 1.5 mL tubes. The lysates were centrifuged at 12,000 rpm for 30 min at 4°C to obtain total protein. After being quantified with a BCA Kit (Thermo Fisher Scientific, MA, USA), 25 μg of protein from each sample was separated by SDS-PAGE and then transferred to PVDF membranes (Millipore, Billerica, MA, USA) in transfer buffer. Next, the membranes were blocked with 5% non-fat milk diluted in TBS solution containing 0.5% Tween-20 (TBST) at 4°C overnight. Then, the membranes were incubated with the following primary antibodies (Abcam, Cambridge, UK) at 4°C overnight: anti-TNIK (1:400 dilution), anti-β-catenin (1:500), anti-pTCF4 (1:500) and anti-Lamin B (1:1000). Finally, the membranes were cultured with horseradish peroxidase-labelled secondary

antibodies (BioTeke, Beijing, China) for 1h at room temperature, followed by the detection with ECL analyses kits (Millipore, Billerica, MA, USA). Finally, chemiluminescent gel imaging system (BIO-RAD Laboratories, Hercules, CA, USA) was used for the quantitative analysis.

RNA extraction and quantitative polymerase chain reaction (qPCR)

Total RNA was isolated from human or mouse tumor tissue samples or cells using a Qiagen miRNeasy kit (Qiagen, Germany) according to the manufacturer's protocol. Subsequently, 1 μg of RNA was subjected to reverse transcription, and single-stranded cDNA was synthesized with the PrimeScript Reagent Kit (Thermo Fisher Scientific, Waltham, MA, USA). Then, qPCR was conducted using a SYBR Green Master Mix kit (Takara Biotechnology, Dalian, China) and performed by CFX96 qPCR machine (Invitrogen, Carlsbad, CA, USA). The relative expression levels were calculated by the $2^{-\Delta\Delta Ct}$ method. U6 and Lamin B served as endogenous references for miR-5590-3p and TNIK, respectively.

Luciferase reporter gene assay

The wild-type (WT) and mutant (MUT) binding sites of TNIK 3'-UTR sequence were inserted into the pmiR-GLO dual-luciferase vector (Promega, WI, USA). Then, the pmiR-GLO-TNIK 3'-UTR recombinant reporter plasmid and miR-5590-3p mimic were co-transfected into HEK-293 cells using Lipofectamine 2000. After 48h of treatment, the luciferase activity of the cells was determined by Multiskan FC Microplate Reader (Thermo Fisher Scientific, Waltham, MA, USA) following the manufacturer's instructions. Renilla signals were normalized to firefly signals. All experiments were performed at least three times.

RNA pull-down assay

RNA samples were labeled with biotin using the Pierce RNA 3' End Desthiobiotinylation Kit (Thermo Fisher Scientific). 50 μL of A2780 cell lysate was respectively incubated with the biotin-labeled miR-5590-3p (Biotin-miR-5590-3p) and Biotin-NC miRNA mimic (Biotin-control) followed by incubation with the streptavidin-coated magnetic beads. 15 μL of cell lysate was used as a loading control (positive control). After incubation for 6 h, the beads were rinsed, and the RNA complex was purified by Trizol, followed by RT-qPCR examination to determine the expression of TNIK mRNA.

Argonaute-2-based RNA immunoprecipitation (RIP) assay

RIP assay was performed with a Magna RIP TM RNA-Binding Protein Immunoprecipitation kit (Millipore). The lysates of A2780 cells were incubated with anti-Argonaute-2 (Anti-Ago2; Millipore) or anti-Immunoglobulin G (Anti-IgG; Millipore, as a negative control). 15 μL of cell lysate was used as a loading control (positive control). Then, the protein A/G beads were added to incubate with the mixture. Finally, the immunoprecipitated RNA was purified and quantified by RT-qPCR using specific primers against miR-5590-3p and TNIK mRNA.

Cell proliferation, migration and invasion assay

Cell proliferation was examined using Cell Counting Kit-8 (Sigma, St. Louis, MO, USA) following the manufacturer's instructions (CCK-8 assay). Briefly, A2780 and OVCAR3 cells were respectively seeded at a density of 10^4 cells/well in 6-well plates, and cell proliferation was assessed by measuring absorbance value at 0, 48 and 72h after transfection. The optical density at 450 nm was detected.

5×10^5 of A2780 or OVCAR3 cells were plated into 6-well plates. On reaching 100% confluence, an nontoxic dose of mitomycin C was used to incubate with the cells for 3 hours and then mitomycin-C was removed by washing before making the scratch. Wounds were scratched onto the monolayer of cells with a 10-μL pipette tip. Then the cells were cultured at 37°C in 5% CO_2 and the images were captured at 0 and 24h respectively.

Transwell assay was conducted to determine the cell invasion by using the transwell plates with 8 μm pore inserts (Millipore, Shijingshan, Haidian, USA). A2780 and OVCAR3 cells (0.5 mL; 2.5×10^4 cells) were placed into the upper sides of the membranes (Matrigel treated)

Table 1. General information of 40 patients with overcila cancer.

Factors	Experimental group (n=40)	Control group (n=40)
Age (years)		
≤54	21	28
>54	19	12
Marital status		
Married	36	35
Unmarried	4	5
Childbearing history		
Yes	32	34
No	8	6
Pathology type		
Mucinous cystadenocarcinoma	11	-
Serous cystadenocarcinoma	19	-
Endometrial carcinoma	7	-
Clear cell carcinoma	3	-
Pathological stage		
I-II	24	-
III-IV	16	-
Degree of differentiation		
High	17	-
Moderate	10	-
Poor	13	-

without FBS, while the lower sides were added with medium plus 10% FBS. 24 hours later, cells on the bottom sides of the membranes were fixed with 4% paraformaldehyde (Takara Biotechnology, Dalian, China) and stained with 0.3% crystal violet solution (Takara Biotechnology, Dalian, China). Finally, every well was photographed under a microscope (Nikon, Chiyoda-Ku, Tokyo, Japan), and the number of stained cells was counted in f randomly selected views of every well.

Tumorigenicity assays in nude mice

Eighty female BALB/c nude mice (weight, 22-24 g; age, 8 weeks; Shanghai SLAC Laboratory Animal Co., Ltd.) were randomly divided into four groups (NC inhibitor, miR-5590-3p inhibitor, miR-5590-3p inhibitor plus Scrambled siRNA, miR-5590-3p inhibitor plus TNIK siRNA). Each mouse was subcutaneously injected with 5×10^6 A2780 cells (suspended in 100 μL of PBS) in the right side of the back of the nude mice to establish the subcutaneous xenograft tumor model. When the tumors reached an average volume of 100 mm^3, each group of mice was intratumorally injected with NC inhibitor, miR-5590-3p inhibitor, miR-5590-3p inhibitor plus Scrambled siRNA or miR-5590-3p inhibitor plus TNIK siRNA at a dosage of 10 mg/Kg every two days until the mice were killed. At week 1, 2, 3 and 4 after injection, 5 mice were selected from each group to check the tumor volume. All of the mice were sacrificed by intraperitoneal injection of sodium pentobarbital (150-200 mg/kg) after 4 weeks to detect the tumor weight. The final volume and weight of each tumor were recorded. The tumor volume (mm^3) was calculated with the formula ($0.5\times Length\times Width^2$).

Statistical analysis

The measurement data are presented as the means ± standard error of mean (SEM) and were analyzed using the statistical software SPSS22.0. At least three independent experiments were carried out for each assay to exclude randomness. Comparison between groups was analyzed by Student's t test or one-way analysis of variance (ANOVA). Pearson correlation coefficient assay was used to evaluate the correlation of miR-5590-3p and TNIK mRNA. $P<0.05$ was considered to indicate a statistically significant difference.

Results

miR-5590-3p is downregulated whereas TNIK is upregulated in OC tissues and OC cells

To explore whether miR-5590-3p was involved in OC, we examined miR-5590-3p and TNIK expression in OC cells and OC tissues. The results showed that miR-5590-3p expression in tumor tissues were significantly lower than matched normal tissues (Fig. 1A). In contrast, the expression of TNIK mRNA was significantly upregulated in tumor tissues compared with the normal tissues (Fig. 1B). The correlation curve showed that the expression level of miR-5590-3p was negatively correlated with the TNIK in OC samples (Fig. 1C, $R^2=0.6931$, $P<0.001$). The expression of miR-5590-3p and TNIK were also investigated in OC cell lines (A2780, SKOV3, HEY, OVCAR3 and IGROV1) and normal human ovarian epithelial cells (HOSEpiC). The results indicated that miR-5590-3p level was reduced in all five OC cell lines compared with those in HOSEpiC cells (Fig. 1D), while TNIK protein had an opposite expression pattern (Fig. 1E). These data suggested that miR-5590-3p might be involved in OC and had a certain relationship with TNIK.

miR-5590-3p suppresses OC cell proliferation, migration and invasion

To investigate the biological function of miR-5590-3p in OC cells, we assessed the effect of miR-5590-3p on cell proliferation and cell invasion in OC cells transfected with NC mimic, miR-5590-3p mimic, NC inhibitor or miR-5590-3p inhibitor in A2780 and OVCAR3 cell lines. The efficiencies of mimic and inhibitor were determined with qPCR assay (Fig. 2A). The CCK-8 assay indicated that cell proliferation was significantly inhibited by miR-5590-3p mimic in A2780 and OVCAR3 (Fig. 2B,C). Next, our results indicated that miR-5590-3p overexpression obviously decreased cell invasion, while miR-5590-3p inhibition showed an opposite effect on A2780 and OVCAR3 cells (Fig. 2D). Wound healing assay also indicated that miR-5590-3p negatively regulated migration of A2780 and OVCAR3 cells (Fig. 2E). These results revealed that miR-5590-3p had a suppressive effect on OC cell proliferation, migration and invasion.

miR-5590-3p translationally inhibits TNIK by targeting specific sequences in the 3'-UTR of TNIK mRNA

To explore the potential mechanism by which miR-5590-3p inhibits OC development, we predicted the miR-5590-3p targets by using the online bioinformatic tool TargetScan (http://www.targetscan.org/vert_71/). The results indicate that miR-5590-3p is likely to interact with the 3'- UTR of TNIK mRNA (Fig. 3A). To verify the post-transcriptionally suppressive activity of miR-5590-3p on TNIK mRNA, we performed a dual-luciferase reporter assay by using WT and mutated TNIK mRNA 3'-UTR reporter vectors. We found that miR-5590-3p mimic significantly decreased the luciferase activity of wild-type TNIK 3'-UTR reporter vector compared with NC mimic, while the Mutant TNIK 3'-UTR reporter vector had no obvious change, which indicated that TNIK was able to bind with miR-5590-3p (Fig. 3B). Moreover, RNA pull-down assay using biotin-labeled miR-5590-3p (biotin-miR-5590-3p) and biotin-NC miRNA mimic (biotin-control)

and Ago-2 based RNA-IP showed that TNIK mRNA was enriched in RNA complexes pulled by biotin-miR-5590-3p, and TNIK mRNA and miR-5590-3p were both enriched in the RNA-protein complexes precipitated by Ago-2 antibody, indicating that miR-5590-3p directly bound with TNIK mRNA (Fig. 3C,D). To further evaluate the effect of miR-5590-3p on TNIK expression, our results suggested that overexpression of miR-5590-3p significantly decreased TNIK expression, whereas inhibition of miR-5590-3p promoted TNIK expression both at mRNA and protein levels (Fig. 3E,F). In addition, TNIK siRNA remarkably decreased TNIK expression at mRNA and protein levels, which exerted a greater inhibitory effect than miR-5590-3p inhibitor (Fig. 3E,F). These results indicated that TNIK was a direct target gene of miR-5590-3p with a negative regulation relationship between them.

Silence of TNIK reverses the effect of miR-5590-3p downregulation on OC cells

To further investigate whether miR-5590-3p regulates behaviors of OC cells through targeting TNIK, we performed rescue experiments to verify whether silence of TNIK could weaken the promoting effect of miR-5590-3p downregulation on proliferation and invasion of A2780 and OVCAR3 cells. Consistent with the previous results, TNIK siRNA decreased TNIK expression at both mRNA and protein levels in A2780 and OVCAR3 cell lines (Fig. 4A,B). Cells were transfected with NC inhibitor, miR-5590-3p inhibitor, miR-5590-3p inhibitor plus Scramble siRNA or miR-5590-3p inhibitor plus TNIK siRNA to conduct the rescue experiments. The results indicated that cell infection with miR-5590-3p inhibitor alone increased cell proliferation, invasion and migration, while co-infection with TNIK siRNA reversed this effect (Fig. 4C-E). These data suggested that TNIK siRNA antagonized the increase of cell proliferation and invasion caused by miR-5590-3p downregulation, which was consistent with its function as a target of miR-5590-3p.

Inhibition of miR-5590-3p promotes the activation of Wnt/β-catenin signaling in OC cells

Previous studies had shown that TNIK was involved in the progression of various cancers by the Wnt/β-

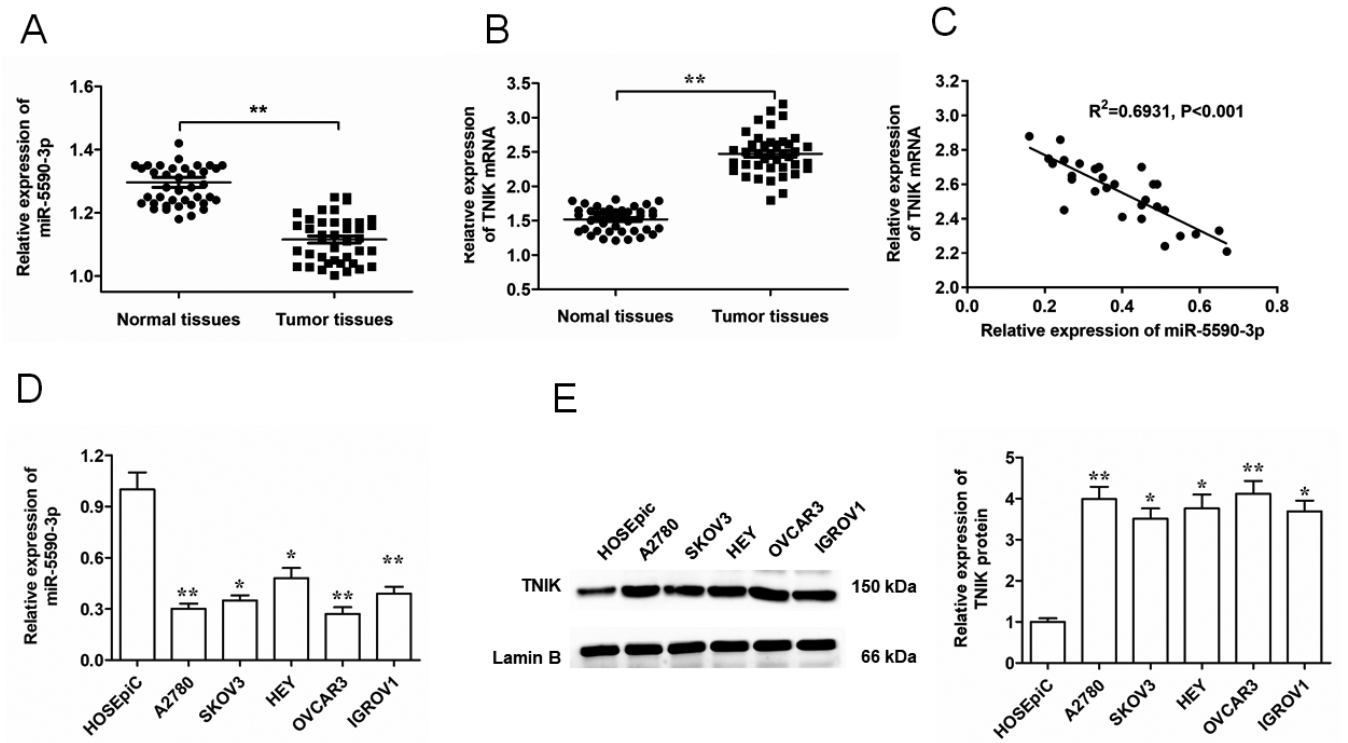

Fig. 1. Expression of miR-5590-3p and TNIK in OC tissues and cell lines. Expression of miR-5590-3p **(A)** and TNIK mRNA **(B)** in 40 OC tissues and matched normal adjacent tissues by qPCR (n=40). **C.** Pearson's correlation curve suggested the negative relation between miR-5590-3p and TNIK in OC tissues. miR-5590-3p **(D)** and TNIK protein **(E)** in OC cell lines (A2780, SKOV3, HEY, OVCAR3, IGROV1) and normal human ovarian epithelial cells (HOSEpiC) (n=3). The data aere presented as the mean ± standard error of mean (SEM), and Student's t test was used for pairwise comparison. Pearson correlation coefficient assay was used to evaluate the correlation of miR-5590-3p and TNIK. **P*<0.05 and ***P*<0.01.

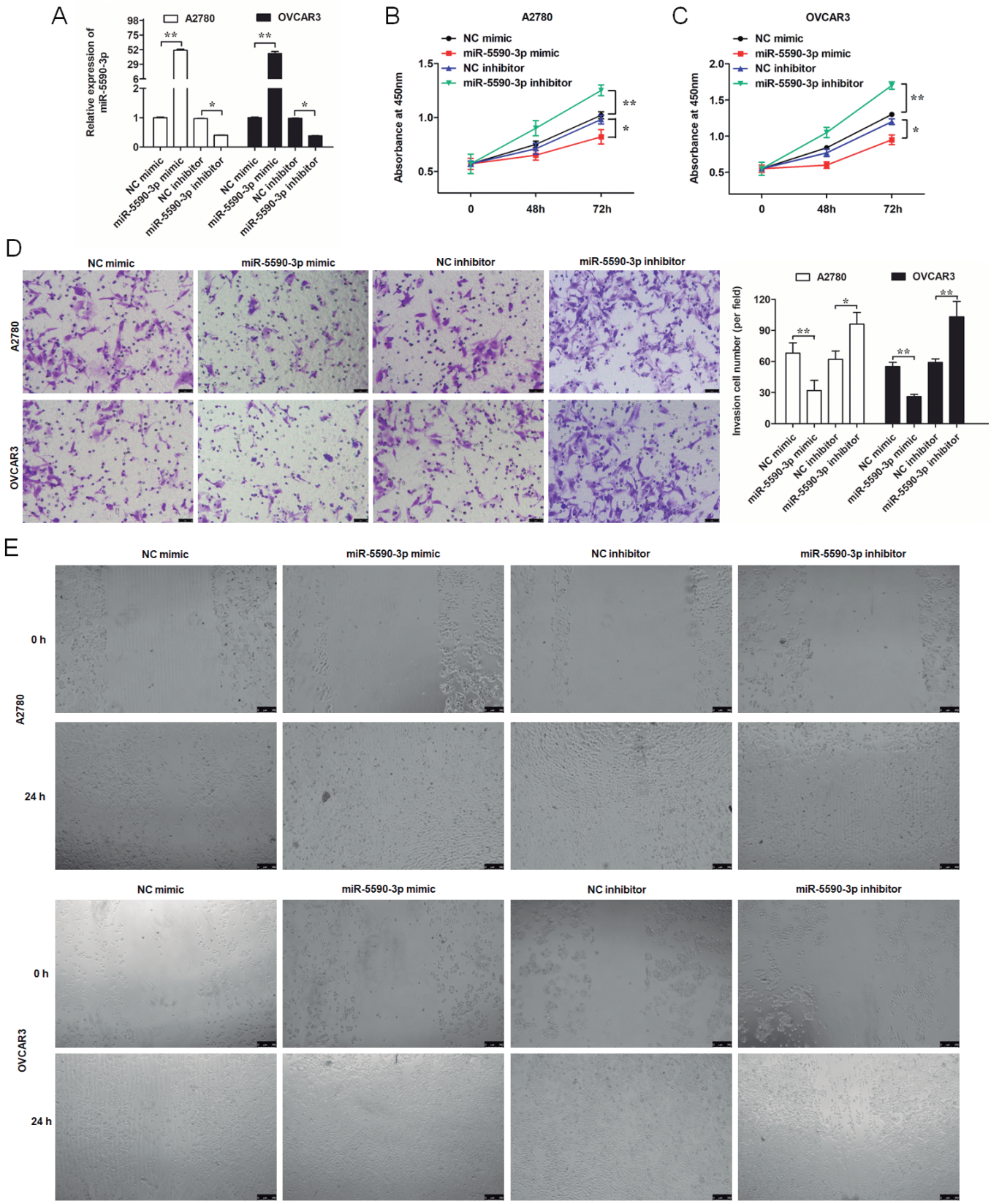

Fig. 2. miR-5590-3p suppresses cell proliferation and cell invasion in OC cells. **A.** Relative expression of miR-5590-3p in A2780 and OVCAR3 cell lines transfected with NC mimic, miR-5590-3p mimic, NC inhibitor or miR-5590-3p inhibitor. Cell proliferation in A2780 **(B)** and OVCAR3 **(C)** cell lines detected by CCK-8 assay at 0h, 48h, and 72h. **D.** Cell invasion of A2780 and OVCAR3 cell lines determined by Transwell assay after 48 h transfection with the indicated oligonucleotides. **E.** Wound healing assay was used to evaluate cell migration capacity. n=3. The data are presented as the mean ± standard error of mean (SEM). Six visual fields were selected to detect cell invasion, and then the average value was taken. Student's t test or one-way analysis of variance (ANOVA) was used for comparisons between groups. **P*<0.05 and ***P*<0.01. × 200.

catenin pathway (Sun et al., 2019; Takahashi et al., 2020; Yan et al., 2022). To explore the underlying molecular mechanisms that miR-5590-3p regulated OC development, we next explored the alteration of Wnt/β-catenin signaling activation in A2780 and OVCAR3 cells. CCK-8 and Transwell assays demonstrated that XAV-939 (a specific inhibitor of the Wnt/β-catenin pathway) significantly inhibited cell proliferation and invasion capabilities compared with DMSO treatment, while these effects were reversed by miR-5590-3p inhibitor or Ad-TNIK (Fig. 5A,B). Together, these results supported that suppression of miR-5590-3p promoted OC cell proliferation and cell invasion by activating the Wnt/β-catenin signaling pathway.

miR-5590-3p suppresses tumor growth in vivo

Finally, to investigate the tumorigenic effects of miR-5590-3p in BALB/C nude mice, we conducted xenograft mouse models by injection of A2780 cells. When tumor volumes reached an average volume of 100 mm^3, mice were injected with miR-5590-3p inhibitor or miR-5590-3p inhibitor plus TNIK siRNA or their negative controls. From our data, the mice infected with miR-5590-3p inhibitor significantly promoted tumor volume (Fig. 6A) and tumor weight (Fig. 6B) compared with the control group. Representative tumor images are shown in Figure 6C. However, silencing TNIK obviously decreased tumor growth (Fig. 6A-C). Then, qPCR assay suggested that miR-5590-3p showed lower expression in miR-5590-3p inhibitor group than the control group (Fig. 6D). Moreover, the expression of TNIK and the activation of the β-catenin pathway in the xenograft tumor was upregulated by transfection with miR-5590-3p inhibitor alone, while co-transfection with TNIK siRNA significantly weakened this promoting effect (Fig. 6E,F).

Discussion

Considering that poor response and recurrence remain the biggest obstacles to improve survival, identifying some new potential strategies for clarifying the underlying mechanism of OC progression is urgently needed. In recent years, increasing evidence suggests that miRNAs may play important regulatory factors in various oncogenic and tumor suppressor pathways (Kan et al., 2015). Our study demonstrated that miR-5590-3p was downregulated in OC tissues and OC cell lines. Downregulation of miR-5590-3p promoted cell proliferation and cell invasion in OC cell lines. TNIK had been proven to be a direct target of miR-5590-3p, and silence of TNIK weakened the promoting effects of miR-5590-3p inhibition on cell proliferation and cell

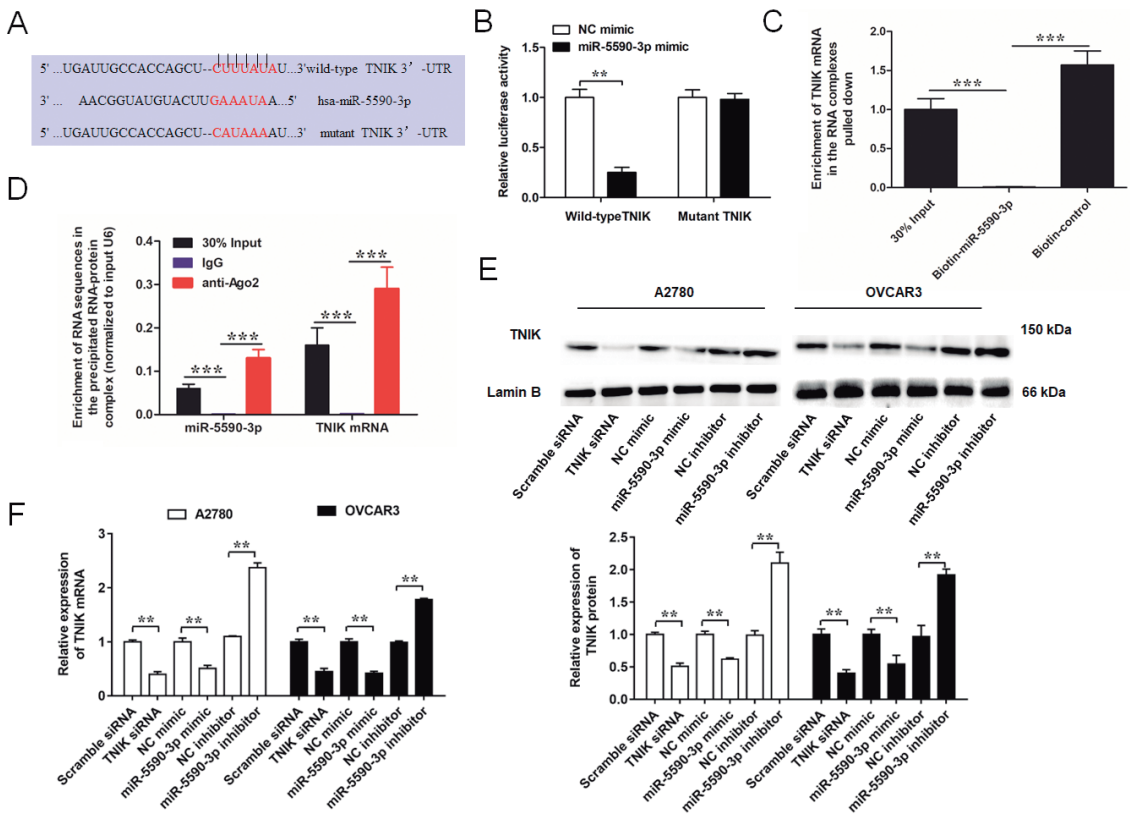

Fig. 3. TNIK is directly targeted by miR-5590-3p. Diagram of the predicted miR-5590-3p binding sites in the 3'-UTR of TNIK mRNA by TargetScan **(A)**. Luciferase reporter assay performed to detect whether miR-5590-3p directly binds to the predicted binding sites in 3'-UTR of TNIK mRNA **(B)**. The effect of miR-5590-3p on TNIK expression detected by qPCR **(C, D)** and Western blotting **(E, F)** in A2780 and OVCAR3 cell lines after 48 h transfection with miR-5590-3p mimic or inhibitor. n=3. The data are presented as the mean ± standard error of mean (SEM) and Student's t test was used for pairwise comparison. **P*<0.05 and ***P*<0.01.

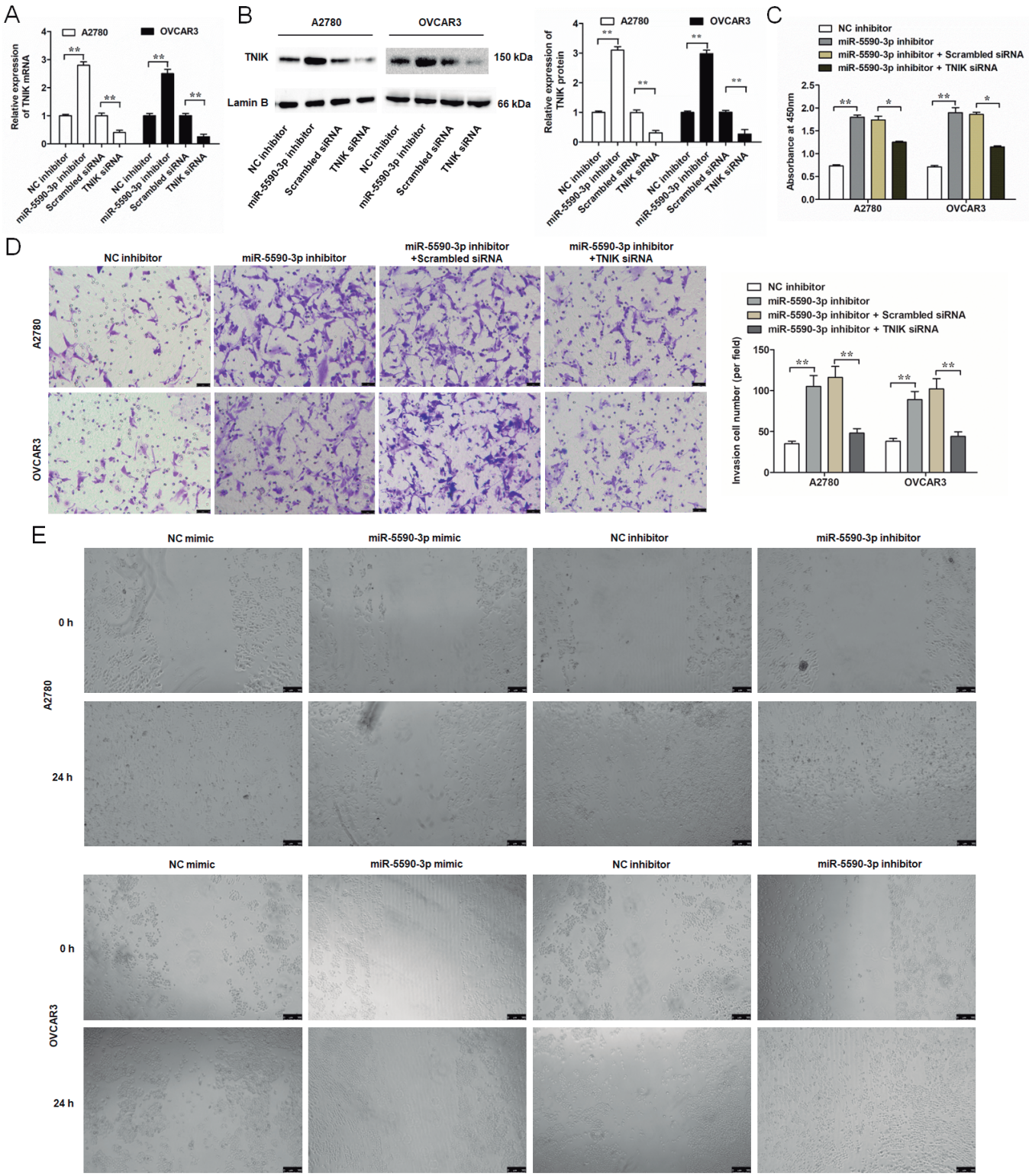

Fig. 4. miR-5590-3p inhibits cell proliferation and invasion by targeting TNIK. Expression of TNIK in A2780 and OVCAR3 cell lines transfected with NC inhibitor, miR-5590-3p inhibitor, scrambled siRNA or TNIK siRNA detected by qPCR **(A)** and Western blotting **(B)**. Cell proliferation, invasion and migration were detected with CCK-8 assay **(C)**, Transwell assay **(D)** and Wound healing **(E)** assays in A2780 and OVCAR3 cell lines after 48h incubation. n=3. The data are presented as the mean ± standard error of mean (SEM). Six visual fields were selected to detect cell invasion, and then the average value was taken. Student's t test was used for pairwise comparison. **P*<0.05 and ***P*<0.01. × 200.

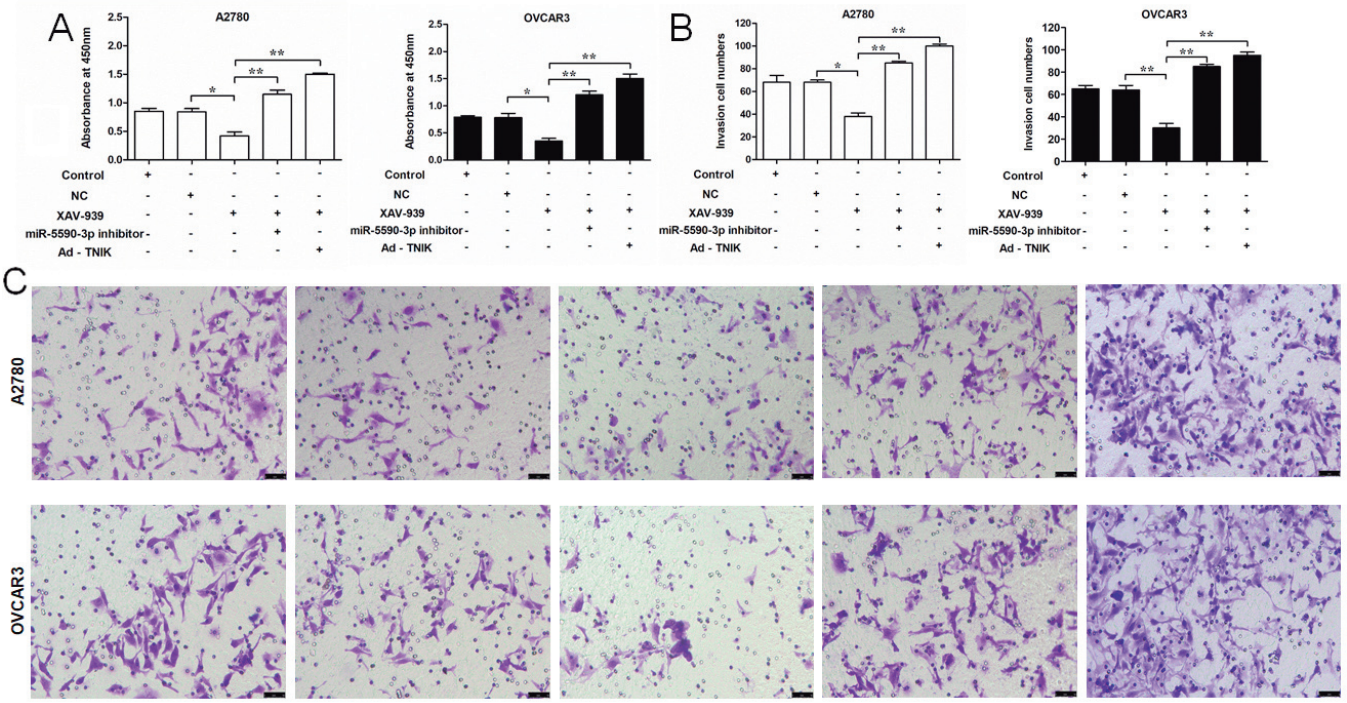

Fig. 5. miR-5590-3p regulates OC cell behaviors through the Wnt/β-catenin signaling pathway. **A.** Western blotting to detect the expression of β-catenin and pTCF4 in A2780 and OVCAR3 cell lines. **B.** Cell proliferation detected by CCK-8 assay. **C.** Cell invasion determined by Transwell assay. All cells were treated with Wnt/β-catenin signaling inhibitor (XAV-939) (1 μM, 12h), and then obtained after 48h transfection with miR-5590-3p inhibitor alone or together with adenoviral TNIK overexpression vector (Ad-TNIK). n=3. The data are presented as the mean ± standard error of mean (SEM) and Student's t test was used for pairwise comparison. **P*<0.05 and ***P*<0.01.

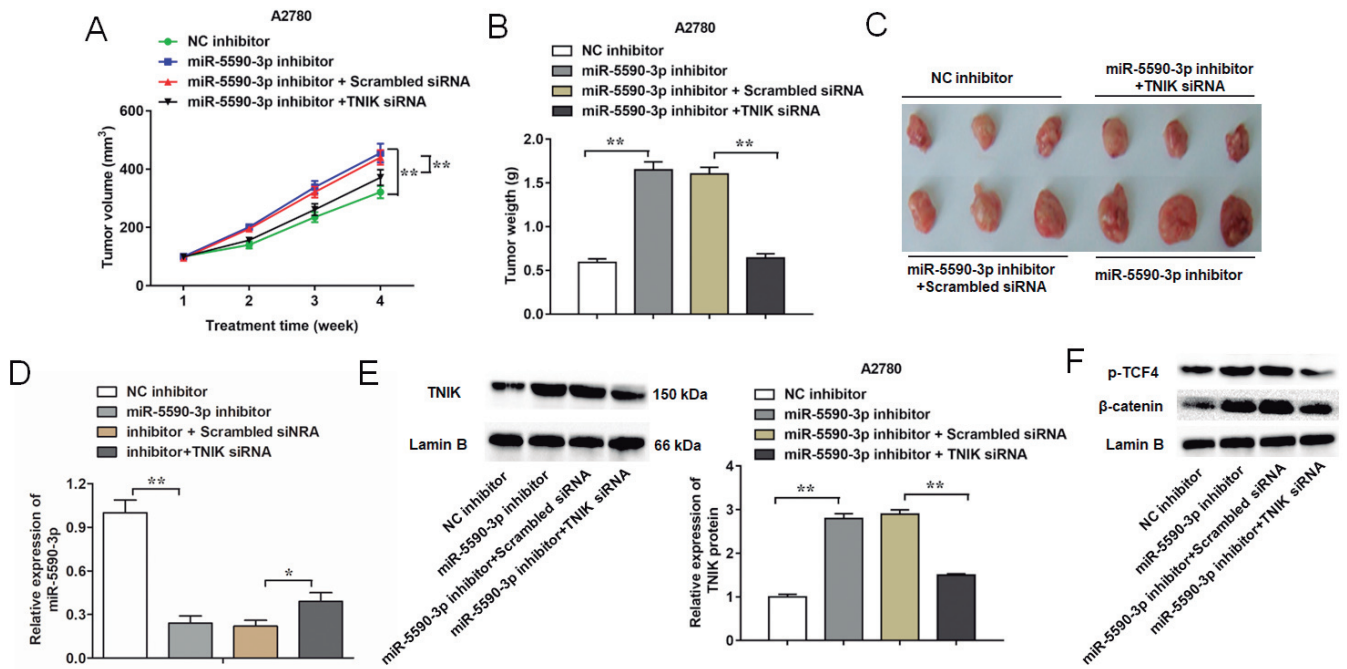

Fig. 6. Inhibition of miR-5590-3p enhances tumor growth *in vivo*. To investigate the tumorigenic effects of miR-5590-3p in BALB/C nude mice, we conducted xenograft mouse models by injection of A2780 cells. **A.** Tumor volume measured weekly after intratumorally injection with NC inhibitor, miR-5590-3p inhibitor, miR-5590-3p inhibitor plus Scrambled siRNA or miR-5590-3p inhibitor plus TNIK siRNA. **B.** Tumor weight of mice intratumorally injected with NC inhibitor, miR-5590-3p inhibitor, miR-5590-3p inhibitor plus Scrambled siRNA or miR-5590-3p inhibitor plus TNIK siRNA. **C.** Representative images of the primary tumors formed in the nude mice after 4 weeks' cultivation. **D.** Expression of miR-5590-3p determined by qPCR. **E, F.** Relative expression of TNIK, p-TCF4 and beta-catenin weas detected by Western blotting assay. The total number of mice is eighty (n=6/group). The data are presented as the mean ± standard error of mean (SEM). Student's t test or one-way analysis of variance (ANOVA) was used for comparisons between groups. **P*<0.05 and ***P*<0.01.

invasion. Our data demonstrated that miR-5590-3p inhibitor exacerbated tumor growth *in vivo*. Thus, our results indicate that the miR-5590-3p/TNIK may function as a tumor suppressor pathway by Wnt/β-catenin signaling pathway.

TNIK is originally identified as a regulator of cytoskeletal organization involved in processes such as cell proliferation, cell motility and cell adhesion. Accordingly, the initial studies focused on the role of TNIK in the regulation of the actin cytoskeleton (Fu et al., 1999; Hu et al., 2004; Taira et al., 2004). Several studies reported that TNIK inhibitors could be treated with Wnt-activated cancers, and increasing evidence demonstrated that TNIK was possible to be developed as agents against several types of human cancers (Ho et al., 2013; Kim et al., 2014). TNIK made TCF4 phosphorylated by directly interacting with β-catenin and TCF4, which lead to the transcriptional activation of Wnt target genes in colorectal cancers (Mahmoudi et al., 2009; Shitashige et al., 2010). Using TNIK siRNA to inhibit TNIK expression and TCF/LEF transcriptional activity was able to suppress colorectal cancer progress (Shitashige et al., 2010). RNA-interference-mediated silencing of TNIK significantly inhibited cell growth and promoted cell death which was involved in AKT activation and cell autophagy in gastric cancer (Yu et al., 2014). Phosphorylated TNIK was overexpressed in hepatocellular carcinoma patients where tumor cells detached, disseminated and finally led to metastasis. These results revealed that high phosphorylated TNIK expression was coincident with tumor progression, which suggested that phosphorylated TNIK could serve as a tumor activator in HCC (Jin et al., 2014). Knockout of TNIK inhibited Wnt/β-catenin signaling and epithelial-mesenchymal transition (EMT), causing early apoptosis via the mitochondrial apoptotic pathway in mammary carcinoma cells (Sun et al., 2019). In addition, siRNA suppressed cell proliferation, induced caspase-dependent apoptosis and inhibited TCF4 phosphorylation in human multiple myeloma (Chon et al., 2016). However, whether TNIK regulates the behaviors of OC cells remains unknown. In this study, we found that TNIK siRNA antagonized the increase of cell proliferation and invasion caused by the inhibition of miR-5590-3p. These results indicated that TNIK functioned as an important regulator for cell behaviors and might be a critical regulator in OC progress.

In recent years, miRNAs have been demonstrated to play important roles in various cancers by regulating their target genes (Biamonte et al., 2019; Wu et al., 2019). In this study, we observed that miR-5590-3p directly targeted TNIK, and inhibition of miR-5590-3p upregulated TNIK, which activated the Wnt/β-catenin signaling pathway. Previous reports showed that TNIK can bind to β-catenin/TCF in the nucleus and activate TCF to drive proliferation in cancer progress (Yu et al., 2014; Sun et al., 2019), which supported our data that inhibition of miR-5590-3p promoted cell proliferation and invasion via TNIK/Wnt/β-catenin pathway in OC cells. In our experiments, we determined that miR-5590-3p inhibition increased expression of TNIK at mRNA and protein levels, which promoted the cell proliferation and invasion. However, overexpression of miR-5590-3p had opposite results. Previous studies demonstrated that miR-5590-3p inhibition activated the Wnt/β−catenin pathway in hepatocellular carcinoma (Zhang et al., 2019), and knockout of TNIK can attenuate Wnt/β-catenin signalling and epithelial-mesenchymal transition (EMT) expression (Sun et al., 2019). Similarly, our results indicated cell proliferation and cell invasion were inhibited by using XAV-939, but miR-5590-3p inhibitor or Ad-TNIK reversed these results, which suggested that miR-5590-3p suppressed the OC progress via the Wnt/β-catenin pathway.

In this study, miR-5590-3p was significantly downregulated in human OC cell lines and patient tissues, and overexpression or inhibition of miR-5590-3p suppressed or promoted cell proliferation and cell invasion. Tumorigenicity assay demonstrated that inhibition of miR-5590-3p promoted tumor volume and weight *in vivo*. Thus, the present study illustrates miR-5590-3p may function as a cancer suppressor gene in OC progression through Wnt/β-catenin signaling by suppressing TNIK expression, which suggests that miR-5590-3p may serve as a potential target for OC treatment.

Acknowledgements. This work was supported by the National Natural Science Foundation of China (Grant No. 81702578).

Availability of data and materials. Not applicable.

Conflict of interest. The authors declare no conflicts of interest.

References

Bakhshmand E.A. and Soltani B.M. (2019). Regulatory effect of hsa-miR-5590-3P on TGFβ signaling through targeting of TGFβ-R1, TGFβ-R2, SMAD3 and SMAD4 transcripts. Biol. Chem. 400, 677-685.

Biamonte F., Santamaria G., Sacco A., Perrone F.M., Di Cello A., Battaglia A.M., Salatino A., Di Vito A., Aversa I., Venturella R., Zullo F. and Costanzo F. (2019). MicroRNA let-7g acts as tumor suppressor and predictive biomarker for chemoresistance in human epithelial ovarian cancer. Sci. Rep. 9, 5668.

Chon H.J., Lee Y., Bae K.J., Byun B.J., Kim S.A. and Kim J. (2016). Traf2- and Nck-interacting kinase (TNIK) is involved in the anti-cancer mechanism of dovitinib in human multiple myeloma IM-9 cells. Amino Acids 48, 1591-1599.

Clevers H. and Nusse R. (2012). Wnt/β-catenin signaling and disease. Cell 149, 1192-1205.

Ford C.E., Henry C., Llamosas E., Djordjevic A. and Hacker N. (2016). Wnt signalling in gynaecological cancers: A future target for personalised medicine? Gynecol. Oncol. 140, 345-351.

Fu C.A., Shen M., Huang B.C., Lasaga J., Payan D.G. and Luo Y. (1999). TNIK, a novel member of the germinal center kinase family that activates the c-Jun N-terminal kinase pathway and regulates the cytoskeleton. J. Biol. Chem. 274, 30729-30737.

Gui J., Yang B., Wu J. and Zhou X. (2011). The enormous influence of

TNIK knockdown on intracellular signals and cell survival. Human Cell 24, 121-126.

Ho K.K., Parnell K.M., Yuan Y., Xu Y., Kultgen S.G., Hamblin S., Hendrickson T.F., Luo B., Foulks J.M., McCullar M.V. and Kanner S.B. (2013). Discovery of 4-phenyl-2-phenylaminopyridine based TNIK inhibitors. Bioorg. Med. Chem. Lett. 23, 569-573.

Hu Y., Leo C., Yu S., Huang B.C., Wang H., Shen M., Luo Y., Daniel-Issakani S., Payan D.G. and Xu X. (2004). Identification and functional characterization of a novel human misshapen/Nck interacting kinase-related kinase, hMINK beta. J. Biol. Chem. 279, 54387-54397.

Jin J., Jung H.Y., Wang Y., Xie J., Yeom Y.I., Jang J.J. and Lee K.B. (2014). Nuclear expression of phosphorylated TRAF2- and NCK-interacting kinase in hepatocellular carcinoma is associated with poor prognosis. Pathol. Res. Pract. 210, 621-627.

Kan C.W., Howell V.M., Hahn M.A. and Marsh D.J. (2015). Genomic alterations as mediators of miRNA dysregulation in ovarian cancer. Genes Chromosomes Cancer 54, 1-19.

Kim J., Moon S.-H., Kim B.T., Chae C.H., Lee J.Y. and Kim S.H. (2014). A novel aminothiazole KY-05009 with potential to inhibit Traf2- and Nck-Interacting Kinase (TNIK) attenuates TGF-β1-mediated epithelial-to-mesenchymal transition in human lung adenocarcinoma A549 Cells. PLoS One 9, e110180.

Liang F., Fu X. and Wang L. (2019). miR-5590-3p-YY1 feedback loop promotes the proliferation and migration of triple-negative breast cancer cells. J. Cell. Biochem. 120, 18415-18424.

Lim L.P., Lau N.C., Philip G.E., Andrew G., Schelter J.M., John C., Bartel D.P., Linsley P.S. and Johnson J.M. (2005). Microarray analysis shows that some microRNAs downregulate large numbers of target mRNAs. Nature 433, 769-773.

Mahmoudi T., Li V.S., Ng S.S., Taouatas N., Vries R.G., Mohammed S., Heck A.J. and Clevers H. (2009). The kinase TNIK is an essential activator of Wnt target genes. EMBO J. 28, 3329-3340.

Majem B., Parrilla A., Jiménez C., Suárez-Cabrera L., Barber M., Marín A., Castellví J., Tamayo G., Moreno-Bueno G., Ponce J., Matias-Guiu X., Alameda F., Romero I., Sánchez J.L., Pérez-Benavente A., Moran S., Esteller M., Reventós J., Rigau M., Gil-Moreno A., Segura M.F. and Santamaría A. (2019). MicroRNA-654-5p suppresses ovarian cancer development impacting on MYC, WNT and AKT pathways. Oncogene 38, 6035-6050.

Marchetti C., Muzii L., Romito A. and Benedetti Panici P. (2019). First-line treatment of women with advanced ovarian cancer: focus on bevacizumab. Onco Targets Ther. 12, 1095-1103.

Niu K., Shen W., Zhang Y., Zhao Y. and Lu Y. (2015). MiR-205 promotes motility of ovarian cancer cells via targeting ZEB1. Gene 574, 330-336.

Ren Y., Shi T., Jiang R., Yin S., Wang P. and Zang R. (2015). Multiple cycles of neoadjuvant chemotherapy associated with poor survival in bulky stage IIIC and IV ovarian cancer. Int. J. Gynecol. Cancer 25, 1398-1404.

Sebastian V., Coward J.I., Bast R.C., Andy B., Berek J.S., Brenton J.D., George C., Crum C.C., Ronny D., Dariush E., Friedlander M., Gabra H., Kaye S.B., Lord C.J., Lengyel E., Levine D.A., McNeish I.A., Menon U., Mills G.B., Nephew K.P., Oza A.M., Sood A.K., Stronach E.A., Walczak H., Bowtell D.D. and Balkwill F.R. (2011). Rethinking ovarian cancer: Recommendations for improving outcomes. Nat. Rev. Cancer 11, 719-725.

Shitashige M., Satow R., Jigami T., Aoki K., Honda K., Shibata T., Ono M., Hirohashi S. and Yamada T. (2010). Traf2- and Nck-interacting kinase is essential for Wnt signaling and colorectal cancer growth. Cancer Res. 70, 5024-5033.

Siegel R.L., Miller K.D. and Jemal A. (2017). Cancer statistics, 2017. Ca Cancer J. Clin. 67, 7-30.

Sun Y., Gao X., Wu P., Wink M., Li J., Dian L. and Liang Z. (2019). Jatrorrhizine inhibits mammary carcinoma cells by targeting TNIK mediated Wnt/β-catenin signalling and epithelial-mesenchymal transition (EMT). Phytomedicine 63, 153015.

Taira K., Umikawa M., Takei K., Myagmar B.E., Shinzato M., Machida N., Uezato H., Nonaka S. and Kariya K. (2004). The Traf2- and Nck-interacting kinase as a putative effector of Rap2 to regulate actin cytoskeleton. J. Biol. Chem. 279, 49488-49496.

Takahashi C., Kondo S., Sadaoka K., Ishizuka S., Noguchi K., Kato Y. and Sugimoto Y. (2020). Effect of TNIK upregulation on JQ1-resistant human colorectal cancer HCT116 cells. Biochem. Biophys. Res. Commun. 530, 230-234.

Tang Z., Li C., Kang B., Gao G., Li C. and Zhang Z. (2017). GEPIA: a web server for cancer and normal gene expression profiling and interactive analyses. Nucleic Acids Res. 45, 98-102.

Wen D., Danquah M., Chaudhary A.K. and Mahato R.I. (2015). Small molecules targeting microRNA for cancer therapy: Promises and obstacles. J. Control. Release 219, 237-247.

Weston C.R. and Davis R.J. (2002). The JNK signal transduction pathway. Curr. Opin. Genet. Dev. 12, 14-21.

Wu J., Miao J., Ding Y., Zhang Y., Huang X., Zhou X. and Tang R. (2019). MiR-4458 inhibits breast cancer cell growth, migration, and invasion by targeting CPSF4. Biochem. Cell. Biol. 97, 722-730.

Wu N., Han Y., Liu H., Jiang M., Chu Y., Cao J., Lin J., Liu Y., Xu B. and Xie X. (2018). MiR-5590-3p inhibited tumor growth in gastric cancer by targeting DDX5/AKT/m-TOR pathway. Biochem. Biophys. Res. Commun. 503, 1491-1497.

Yan R., Zhu H., Huang P., Yang M., Shen M., Pan Y., Zhang C., Zhou X., Li H., Ke X., Zhang W., Hao P., Qu Y. (2022). Liquidambaric acid inhibits Wnt/β-catenin signaling and colon cancer via targeting TNF receptor-associated factor 2. Cell Rep. 38, 110319.

Yu D.H., Zhang X., Wang H., Zhang L., Chen H., Hu M., Dong Z., Zhu G., Qian Z., Fan J., Su X., Xu Y., Zheng L., Dong H., Yin X., Ji Q. and Ji J. (2014). The essential role of TNIK gene amplification in gastric cancer growth. Oncogenesis 2, e89.

Zhang W., Wu Y., Hou B., Wang Y., Deng D., Fu Z. and Xu Z. (2019). A SOX9-AS1/miR-5590-3p/SOX9 positive feedback loop drives tumor growth and metastasis in hepatocellular carcinoma through the Wnt/β-catenin pathway. Mol. Oncol. 13, 2194-2210.

Accepted June 5, 2023